JOURNAL OF COMPUTATIONAL PHYSICS **118**, 131–151 (1995)

Support-Operator Finite-Difference Algorithms for General Elliptic Problems*

MIKHAIL SHASHKOV

T-7, MS-B284, Los Alamos National Laboratory, Los Alamos, New Mexico 87545

AND

STANLY STEINBERG

Department of Mathematics and Statistics, University of New Mexico, Albuquerque, New Mexico 87131

Received August 27, 1993; revised October 24, 1994

An algorithm is developed for discretizing boundary-value problems given by a general linear elliptic second-order partial-differential equation with general mixed or Robin boundary conditions in general logically rectangular grids. The continuum problem can be written as an operator equation where the operator is self adjoint and positive definite. The discrete approximations have the same property. Consequently, the matrices for the discrete problem are symmetric and positive definite. Also, the scheme has a nearest neighbor stencil. Consequently, the most powerful linear solvers can be applied. In smooth grids, the algorithm produces second-order accurate solutions. It is the generality of the problem (general matrix coefficients, general boundary conditions, general logically rectangular grids) that makes finding such an algorithm difficult. The algorithm, which is a combination of the method of support operators and the mapping method, overcomes certain difficulties of the individual methods, producing a high-quality algorithm for solving general elliptic problems. © 1995 Academic Press, Inc.

1. INTRODUCTION

This paper considers the problem of accurately solving boundary-value problems which consist of a general elliptic partial-differential equation (PDE)

$$-\mathbf{div}\ \mathbf{K}\ \mathbf{grad}\ u = f, \tag{1}$$

given in some region Ω, and a general mixed boundary condition (BC)

$$\beta(\vec{\mathbf{n}}, \mathbf{K}\ \mathbf{grad}\ u) + \alpha u = \gamma, \tag{2}$$

given on the boundary $\partial\Omega$ of Ω (here $(\vec{A}, \vec{B})$ is the inner product of two vectors). The problem is to solve for the function u when $\mathbf{K}$ is a given matrix or tensor function of the spatial variables that is symmetric and positive definite, f is a source term that is a function of the spatial variables, $\vec{\mathbf{n}}$ is a unit outward normal to $\partial\Omega$, and α, β, and γ are functions given on $\partial\Omega$. It is assumed that $\alpha\beta \geq 0$.

In this paper, we derive a second-order accurate, nearest neighbor approximation for the boundary-value problem consisting of the PDE (1) and the BC (2) which preserves the main operator properties of the continuum problem. The boundary-value problem considered here can be written in terms of an operator that is self-adjoint and positive definite (see Section 2). Our approximation to this boundary-value problem preserves this property; that is, the approximation can be written in terms of a symmetric and positive-definite matrix. One reason these properties are important is because the most powerful linear solvers can be used to invert such matrices.

Our study of elliptic problems is motivated by the desire to solve more realistic problems that involve complex systems of partial differential equations and complex geometry. It is common for an elliptic problem to appear naturally in such problems and it is critical to have a good discretization for this operator.

The solution algorithm for the elliptic problem is derived by combining two methods: the method of support operators as developed by Favorskii *et al.* [9], and the mapping method, see for instance Thompson *et al.* [12]. There is also a discussion of the mapping method in Knupp and Steinberg [6] that is particularly appropriate to this discussion. The support-operator method proceeds by deriving definitions of the divergence, gradient, and curl that satisfy certain integral identities. In this method the grid is viewed as a set of points in physical space that can be arranged in a rectangular array so that the neighbors of a point in physical space are the same as the neighbors in

* The research on which this report is based was financed in part by the U.S. Department of Energy through the New Mexico Waste-Management Education and Research Consortium (WERC) and Sandia National Laboratories, by the Department of Energy under Contract DE-AC04-76DP00789, for which Dr. M. G. Marietta was the technical monitor, and by the Schlumberger Foundation. Dr. Shashkov was partially supported by the independent research and development program at Ecodynamics Research Associates.

0021-9991/95 $6.00

the array. In the mapping method, the grid is given as the image of a simple rectangular grid in logical space, under a transformation that maps logical space to physical space. Then the chain rule is then used to transform the PDE and BC to logical space where they are discretized.

These methods are combined by first applying the mapping method to the boundary-value problem (1) and (2). To apply this method it is assumed that there exists a mapping of the region Ω to a square. The boundary value is then transformed to the square using this mapping. An important point here is that the transformed problem has exactly the same form as the original problem. The coefficients in the PDE and the BC do change, but the new K is still symmetric and positive definite. Next, the support operators method is used to discretize the transformed problem on a uniform grid. The resulting scheme is shown to have all of the desired properties. The second-order accuracy of the method is demonstrated numerically.

This combination of methods produces a new algorithm for solving boundary-value problems for general elliptic operators with general Robin boundary conditions, in general regions. The discretization uses logically rectangular grids and a natural staggered discretization for vector fields. The approximations are second-order accurate with nearest neighbor stencils. The matrix related to the discrete problem is symmetric and positive definite.

We note that neither the support operators nor the mapping method, by themselves, give all of the desired properties. In the support-operators method, the discrete gradient is not local when the grid is non-orthogonal and when a local basis system is used to describe the vector field (see [9] and Section 4 of this paper). The source of the non-locality is the use of a local basis of normal components to cell faces to describe vectors. A non-local gradient means that the matrices of the discrete gradient and Laplacian operators are not banded. In fact, the gradient is given by the inverse of a banded matrix times a banded matrix (see Section 4). If this algorithm is restricted to a rectangular grid, then the gradient is local and, in fact, has a nearest neighbor stencil. On the other hand, the matrices resulting from the mapping method are not symmetric for second-order approximation of general Robin boundary conditions unless the matrix $\mathbf{K}$ is diagonal and the grid is a product of one-dimensional grids.

In Section 2 the properties of the continuum problem are described. In Section 3 the support-operators method for a rectangular grid is described, while in Section 4 the support-operators method is extended to logically rectangular grids for problems with diagonal K. The mapping method and the combination of the two methods are described in Section 5. The results of the numerical tests are given in Section 6.

2. PROPERTIES OF THE CONTINUUM PROBLEM

In this section the properties of the continuum boundary-value problem in two dimensions (x, y) are explicitly derived in preparation for the discretization process. It is assumed that all functions are smooth enough that all definitions make sense. Thus, precise definitions of function spaces are not given.

First, note that the PDE (1) can be interpreted as a stationary heat equation for which there is only one conservation law—the law of heat conservation:

$$\frac{dQ}{dt} = -\oint_S (\vec{w}, \vec{n})\, dS \tag{3}$$

where

$$Q = \int_V u\, dV, \qquad \vec{w} = -\mathbf{K}\,\mathbf{grad}\, u \tag{4}$$

are the total amount of heat and heat flux. Formally, this relation can be obtained from the integral identity

$$\int_V \mathbf{div}\, \vec{w}\, dV = \oint_S (\vec{w}, \vec{n})\, dS \tag{5}$$

as follows:

$$\frac{dQ}{dt} = \frac{d}{dt}\int_V u\, dV = -\int_V \mathbf{div}\, \vec{w}\, dV = -\oint_S (\vec{w}, \vec{n})\, dS. \tag{6}$$

More generally, the differential operator $-\mathbf{div}\ \mathbf{K}\ \mathbf{grad}$ is self adjoint and positive. As shown below, this property follows from the integral identity

$$\int_V \phi\, \mathbf{div}\, \vec{w}\, dV + \int_V (\vec{w}, \mathbf{grad}\, \phi)\, dV = \oint_S \phi(\vec{w}, \vec{n})\, dS, \tag{7}$$

which connects the operators **div** and **grad**. When deriving a finite-difference scheme, it is important to preserve the difference analog of integral identities (5) and (7).

In the version of the support-operator method used in this paper, the natural invariant definition of the divergence operator,

$$\mathbf{div}\, \vec{w} = \lim_{V\to 0} \frac{1}{V}\oint_V (\vec{w}, \vec{n})\, dV, \tag{8}$$

is used to derive a discrete analog **DIV** of the divergence **div**, and then the integral identity (7) is used to derive a definition of a discrete analog **GRAD** of the gradient **grad**.

2.1. *The Second-Order Operator*

First the important properties of the second-order operator are derived directly from an integral identity. The case of Dirichlet boundary conditions for the BVP consisting of (1) and (2) is easy to analyze, so here we concentrate on the mixed BC; that is, choose $\beta = 1$. Thus the problem to be analyzed is

$$\begin{aligned} -\mathbf{div}\,\mathbf{K}\,\mathbf{grad}\, u &= f, & (x,y) &\in V, \\ (\mathbf{K}\,\mathbf{grad}\, u, \vec{n}) + \alpha u &= \psi, & (x,y) &\in \partial V, \alpha \geq 0, \end{aligned} \tag{9}$$

where the function u belongs to space H with the following inner product:

$$(u,v)_H = \int_V uv\, dV + \oint_{\partial V} uv\, dS, \qquad u, v \in H. \tag{10}$$

Equation (9) can be written in operator form

$$\mathbf{A}u = \mathbf{F} \tag{11}$$

where the operator $\mathbf{A}$ is given by

$$\mathbf{A}: H \to H, \qquad \mathbf{A}u = \begin{cases} -\mathbf{div}\,\mathbf{K}\,\mathbf{grad}\, u, & (x,y) \in V, \\ (\mathbf{K}\,\mathbf{grad}\, u, \vec{n}) + \alpha u, & (x,y) \in \partial V, \end{cases} \tag{12}$$

and the right-hand side has the form

$$\mathbf{F} = \begin{cases} f, & (x,y) \in V \\ \psi, & (x,y) \in \partial V \end{cases}. \tag{13}$$

The operator $\mathbf{A}$ has the following properties:

$$(\mathbf{A}u, v)_H = (u, \mathbf{A}v)_H, \qquad (\mathbf{A}u, u)_H \geq 0, \tag{14}$$

and, moreover,

$$(\mathbf{A}u, u)_H > 0, \qquad \text{if } \alpha > 0. \tag{15}$$

The proof of these properties relies on the definition of the operator (12), the inner product (10), and an application of the integral identity (7):

$$(\mathbf{A}u, v)_H = \int_V (\mathbf{K}\,\mathbf{grad}\, u, \mathbf{grad}\, v)\, dV + \oint_{\partial V} \alpha uv\, dS. \tag{16}$$

This relationship implies that $\mathbf{A}$ is a symmetric operator. If v is taken to be equal to u in the previous equation (16), then

$$(\mathbf{A}u, u)_H = \int_V (\mathbf{K}\,\mathbf{grad}\, u, \mathbf{grad}\, u)\, dV + \oint_{\partial V} \alpha u^2\, dS \geq 0, \tag{17}$$

that is, $\mathbf{A}$ is positive because $\mathbf{K}$ is positive.

2.2. *The First-Order Operators*

The properties of the second-order operator can be derived from those of the divergence and gradient. Moreover, the properties of the divergence and gradient are of interest in their own right. To investigate the properties of first-order operators, the space of vector functions $\mathbf{H}$ must be defined. For two vector functions $\vec{A}, \vec{B} \in \mathbf{H}$, their inner product is defined as

$$(\vec{A}, \vec{B})_{\mathbf{H}} = \int_V (\vec{A}, \vec{B})\, dV. \tag{18}$$

For the next calculation, it is useful to rewrite original equations (9) in flux form:

$$\begin{aligned} \mathbf{div}\, \vec{w} &= f, & (x,y) &\in V, \\ \vec{w} &= -\mathbf{K}\,\mathbf{grad}\, u, & (x,y) &\in V, \\ -(\vec{w}, \vec{n}) + \alpha u &= \psi, & (x,y) &\in \partial V. \end{aligned} \tag{19}$$

From the flux form (19), it is clear that operator $\mathbf{A}$ can be represented in the form

$$\mathbf{A} = \mathbf{BKC} + \mathbf{D} \tag{20}$$

where the operators $\mathbf{B}$, $\mathbf{K}$, $\mathbf{C}$, and $\mathbf{D}$ have the definitions

$$\mathbf{C}u = -\mathbf{grad}\, u, \qquad (x,y) \in V, \tag{21}$$

$$\mathbf{K}\vec{w} = \mathbf{K}\,\vec{w}, \qquad (x,y) \in V, \tag{22}$$

$$\mathbf{B}\vec{w} = \begin{cases} +\mathbf{div}\, \vec{w}, & (x,y) \in V \\ -(\vec{w}, \vec{n}), & (x,y) \in \partial V \end{cases}, \tag{23}$$

$$\mathbf{D}u = \begin{cases} 0, & (x,y) \in V \\ \alpha u, & (x,y) \in \partial V \end{cases}, \tag{24}$$

where

$$\mathbf{C}: H \to \mathbf{H},$$
$$\mathbf{K}: \mathbf{H} \to \mathbf{H},$$
$$\mathbf{B}: \mathbf{H} \to H,$$
$$\mathbf{D}: H \to H.$$

The next step is to show that

$$\mathbf{B} = \mathbf{C}^*. \tag{25}$$

The definition of operator $\mathbf{B}$, the formula (10) for the inner product in the space H, and integral identity (7) which connects **div** and **grad** give

$$\begin{aligned} (\mathbf{B}\vec{w}, u)_H &= \int_V u\, \mathbf{div}\, \vec{w}\, dV - \oint_{\partial V} u(\vec{w}, \vec{n})\, dS \\ &= -\int_V (\vec{w}, \mathbf{grad}\, u)\, dV \\ &= (\vec{w}, \mathbf{C}u)_{\mathbf{H}}, \end{aligned} \tag{26}$$

which is what is required. The statement of the original problem gives

$$\mathbf{K} = \mathbf{K}^* > 0. \tag{27}$$

Also, the required properties of the operator **D** follow from

$$(\mathbf{D}u, v)_H = \oint_{\partial V} \alpha uv \, dS = (u, \mathbf{D}v)_H, \tag{28}$$

and

$$(\mathbf{D}u, u)_H = \oint_{\partial V} \alpha u^2 \, dS \geq 0, \tag{29}$$

because $\alpha \geq 0$.

This means that

$$\mathbf{A} = \mathbf{C}^*\mathbf{K}\mathbf{C} + \mathbf{D}, \tag{30}$$

and then properties (14) of operator **A** follow from the properties of operators **B**, **K**, **C**, and **D**:

$$\mathbf{B} = \mathbf{C}^*, \qquad \mathbf{D} = \mathbf{D}^* \geq 0, \qquad \mathbf{K} = \mathbf{K}^* > 0. \tag{31}$$

In particular, note that if **A** kills u, then

$$\begin{aligned} 0 &= (\mathbf{A}u, u) \\ &= (\mathbf{C}^*\mathbf{K}\mathbf{C}u + \mathbf{D}u, u) \\ &= (\mathbf{K}\mathbf{C}u, \mathbf{C}u) + (\mathbf{D}u, u). \end{aligned} \tag{32}$$

Because $\mathbf{D} \geq 0$ and $\mathbf{K} > 0$, this implies that $\mathbf{C}u = -\mathbf{grad}\, u = 0$, that is, u is a constant. If α is positive at some point on the boundary then $u = 0$ and then **A** is positive definite.

These considerations, in continuous case, illuminate the properties of first-order operators that must be preserved when the finite-difference schemes are constructed.

3. THE SUPPORT-OPERATORS METHOD

An overview of the method of support operators, as developed by Favorskii *et al.* [9], is given and then applied to the elliptic boundary-value problem. The prime operator is chosen as the divergence **div** and its discretization **DIV** is chosen as a discrete analog of the invariant definition (8) of the divergence operator. The derived operator is the gradient **grad** whose discrete analog is **GRAD**. The discretization of the elliptic equation (1) is then given by

TABLE I

Continuum and Discrete Notation

Cont.	Disc.	Cont.	Disc.
u	U	f	F
div	**DIV**	**grad**	**GRAD**
H	HC	**H**	$\mathcal{HS}$
A	$\mathcal{A}$	**K**	$\mathcal{K}$
B	$\mathcal{B}$	**D**	$\mathcal{D}$
α	Υ	ψ	Ψ

$$\mathbf{DIV}\ K\ \mathbf{GRAD}\ U = F, \tag{33}$$

where K, U, and F are discretizations of **K**, u, and f given in the PDE (1) (again, see Table I for the notation).

3.1. *Main Stages*

The five main stages in the support-operators method of constructing conservative difference schemes for elliptic PDEs are:

1. Write the differential equations in terms of the invariant first-order differential operators **div** and **grad**.
2. Choose where in the grid the scalar and vector functions are to be located.
3. Choose one of the operators **div** and **grad** to be the *prime* operator.
4. Choose a discretization of the prime operator.
5. The discretization for the remaining operator, called the *derived* operator, is derived from the discretization of the prime operator and a difference analog of the integral identity (7).

3.2. *Spaces of Discrete Functions*

In this section, the support-operators scheme in a simple rectangular grid in two dimensions is constructed following the outline in the previous section. A rectangular grid with constant steps hX and hY in x and y directions is used (see Fig. 1). The nodes of this grid are given by pairs of indices (i, j), $1 \leq i \leq N$, $1 \leq j \leq M$. For cells, integer indices are also used; a cell has the same indices as its southwest corner (see Fig. 1).

The discrete analog of a scalar function u is a cell centered scalar function $U_{(i,j)}$ (see Fig. 1), while the analog of a vector function $\vec{w}$ is a discrete vector function $\vec{W} = (WX, WY)$ where $WX_{(i,j)}$ is located at the center of the left vertical side of cell (i, j) and $WY_{(i,j)}$ is located at the center of the bottom side of cell (i, j) (see Fig. 2). The treatment of the boundary conditions requires the introduction of the value of the scalar function on the centers of the boundary segments (see Fig. 1): $U_{(0,j)}$, $U_{(N,j)}$,

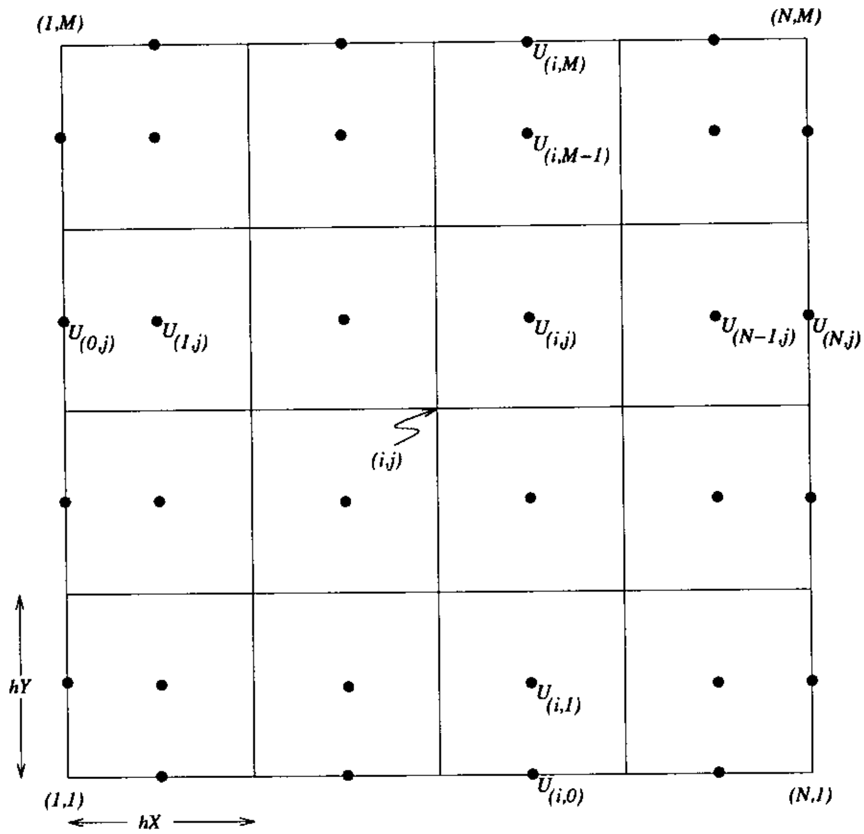

FIG. 1. Discretization of scalar.

$j = 1, ..., M-1$, and $U_{(i,1)}$, $U_{(i,M)}$, $i = 1, ..., N-1$. See Table I for a summary of the notation.

The space of discrete scalar functions is labeled HC and has the inner product

$$(U, V)_{HC} = \sum_{i=1}^{N-1}\sum_{j=1}^{M-1} U_{(i,j)}V_{(i,j)}hXhY + \sum_{i=1}^{N-1} U_{(i,0)}V_{(i,0)}hX + \sum_{j=1}^{M-1} U_{(N,j)}V_{(N,j)}hY + \sum_{i=1}^{N-1} U_{(i,M)}V_{(i,M)}hX + \sum_{j=1}^{M-1} U_{(0,j)}V_{(0,j)}hY. \quad (34)$$

The space of vector functions is labeled $\mathcal{HS}$ and has the inner product

$$(\vec{A}, \vec{B})_{\mathcal{HS}} = \sum_{i=1}^{N-1}\sum_{j=1}^{M-1} (\vec{A}, \vec{B})_{(i,j)}hXhY, \quad (35)$$

where

$$\begin{aligned}(\vec{A}, \vec{B})_{(i,j)} &= \tfrac{1}{4}\{(AX_{(i,j)}BX_{(i,j)} + AY_{(i,j)}BY_{(i,j)}) \\ &\quad + (AX_{(i,j)}BX_{(i,j)} + AY_{(i,j+1)}BY_{(i,j+1)}) \\ &\quad + (AX_{(i+1,j)}BX_{(i+1,j)} + AY_{(i,j+1)}BY_{(i,j+1)}) \\ &\quad + (AX_{(i+1,j)}BX_{(i+1,j)} + (AY_{(i,j)}BY_{(i,j)})\} \\ &= \tfrac{1}{2}\{AX_{(i,j)}BX_{(i,j)} + AX_{(i+1,j)}BX_{(i+1,j)} \\ &\quad + AY_{(i,j)}BY_{(i,j)} + AY_{(i,j+1)}BY_{(i,j+1)}\}.\end{aligned} \quad (36)$$

This definition takes into account the fact that the components of the discrete vectors are not located at the same point.

3.3. *The Prime Operator*

The continuum prime operator is the divergence **div** along with some boundary conditions:

$$\mathbf{B}\vec{w} = \begin{cases} \mathbf{div}\,\vec{w}, & (x, y) \in V, \\ -(\vec{w}, \vec{n}), & (x, y) \in \partial V. \end{cases} \quad (37)$$

The approximation $\mathcal{B}\colon \mathcal{HS} \to HC$ of the prime operator $\mathbf{B}$ is obtained by using its invariant definition in the cell (i, j) as in

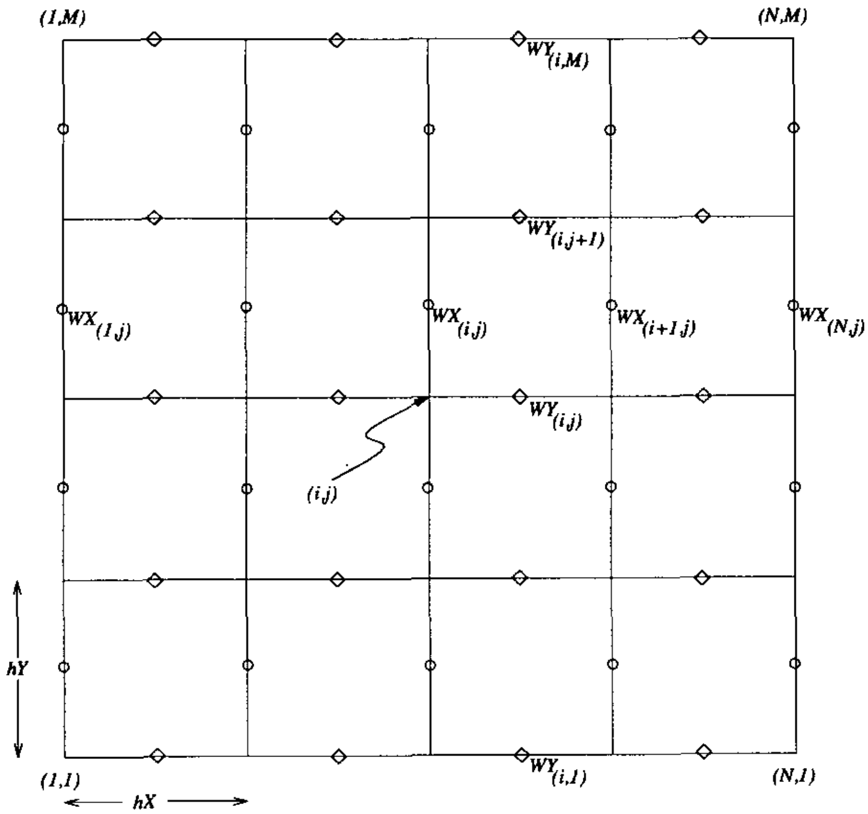

FIG. 2. Discretization of a vector.

definition (8):

$$(\mathcal{B}\vec{W})_{(i,j)} = \begin{cases} \dfrac{WX_{(i+1,j)} - WX_{(i,j)}}{hX} + \dfrac{WY_{(i,j+1)} - WY_{(i,j)}}{hY}, & i = 1, \dots, N-1, \; j = 1, \dots, M-1, \\ -WY_{(i,1)}, & i = 1, \dots, N-1, j = 0, \\ +WY_{(i,M)}, & i = 1, \dots, N-1, j = M, \\ -WX_{(1,j)}, & i = 0, j = 1, \dots, M-1, \\ +WX_{(N,j)}, & i = N, j = 1, \dots, M-1, \end{cases} \quad (38)$$

$$\begin{aligned} (\mathcal{C}^{(x)}U)_{(i,j)} &= \frac{U_{(i,j)} - U_{(i-1,j)}}{hX}, && i = 2, \dots, N-1, j = 1, \dots, M, \\ (\mathcal{C}^{(x)}U)_{(1,j)} &= \frac{U_{(1,j)} - U_{(0,j)}}{hX/2}, && j = 1, \dots, M, \\ (\mathcal{C}^{(x)}U)_{(N,j)} &= \frac{U_{(N,j)} - U_{(N-1,j)}}{hX/2}, && j = 1, \dots, M, \\ (\mathcal{C}^{(y)}U)_{(i,j)} &= \frac{U_{(i,j)} - U_{(i,j-1)}}{hY}, && i = 1, \dots, N, j = 2, \dots, M-1, \\ (\mathcal{C}^{(y)}U)_{(i,1)} &= \frac{U_{(i,1)} - U_{(i,0)}}{hY/2}, && i = 1, \dots, N, \\ (\mathcal{C}^{(y)}U)_{(i,M)} &= \frac{U_{(i,M)} - U_{(i,M-1)}}{hY/2}, && i = 1, \dots, N. \end{aligned} \quad (39)$$

3.4. *The Derived Operator*

The derived operator $\mathcal{C}$: $HC \to \mathcal{HS}$ is the adjoint of $\mathcal{B}$, $\mathcal{C} = \mathcal{B}^*$, and then **GRAD** $= -\mathcal{C}$ is the analog of **grad**. A formula for $\mathcal{C}$ is derived using a discrete analog of the integral identity (7). Using the previous expression (38) for the operator $\mathcal{B}$, the definition of the inner products for spaces HC (34) and $\mathcal{HS}$ (35) and a bit of algebra gives:

Recall that the continuum gradient has the property that if the gradient of a function is zero, then the function is constant. An important property of the discrete gradient is that it mimics this property. If **GRAD** $U = 0$, then U is a constant. In fact, $(\mathcal{C}^{(x)}U) = 0$ implies that U is constant along rows and $(\mathcal{C}^{(y)}U) = 0$ implies that U is constant along columns.

3.5. *Multiplication by a Matrix and the Operator* $\mathcal{D}$

In two dimensions, the matrix **K** has the form

$$\mathbf{K} = \begin{pmatrix} K_{xx} & K_{xy} \\ K_{xy} & K_{yy} \end{pmatrix} \tag{40}$$

and its discrete analog has the form

$$\mathcal{K} = \begin{pmatrix} KXX & KXY \\ KXY & KYY \end{pmatrix}. \tag{41}$$

The values $KXX_{(i,j)}$ and $KYY_{(i,j)}$ are taken at the same points, respectively, as are $WX_{(i,j)}$ and $WY_{(i,j)}$. The value of $KXY_{(i,j)}$ is taken at the cell center (see Fig. 3). If the standard averaging notation is introduced for the components of a vector $\vec{A} = (AX, AY)$,

$$AX_{(i+1/2,j)} = \frac{AX_{(i+1,j)} + AX_{(i,j)}}{2}, \qquad AY_{(i,j+1/2)} = \frac{AY_{(i,j+1)} + AY_{(i,j)}}{2}, \tag{42}$$

and so forth, then the components of $\mathcal{K}\vec{A}$ are defined by

$$\begin{aligned}
(\mathcal{K}\vec{A})^X_{(i,j)} &= KXX_{(i,j+1/2)}AX_{(i,j)} \\
&\quad + \tfrac{1}{2}KXY_{(i-1/2,j+1/2)}AY_{(i-1,j+1/2)} \\
&\quad + \tfrac{1}{2}KXY_{(i+1/2,j+1/2)}AY_{(i,j+1/2)}, \\
(\mathcal{K}\vec{A})^X_{(1,j)} &= KXX_{(1,j+1/2)}AX_{(1,j)} \\
&\quad + KXY_{(3/2,j+1/2)}AY_{(1,j+1/2)}, \\
(\mathcal{K}\vec{A})^X_{(N,j)} &= KXX_{(N,j+1/2)}AX_{(N,j)} \\
&\quad + KXY_{(N-1/2,j+1/2)}AY_{(N-1,j+1/2)},
\end{aligned} \tag{43}$$

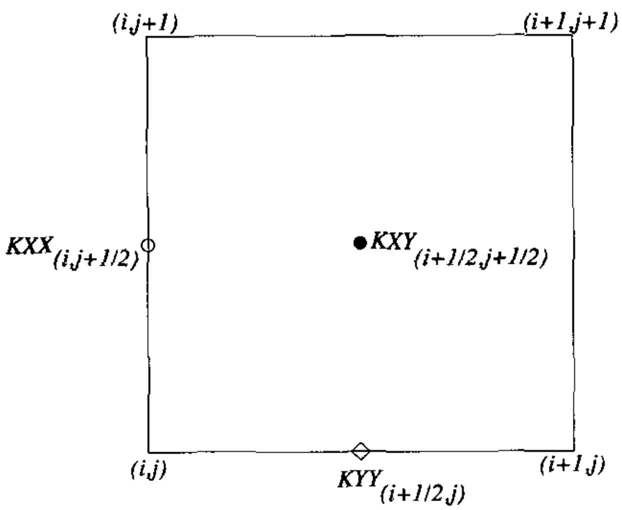

FIG. 3. Matrix discretization.

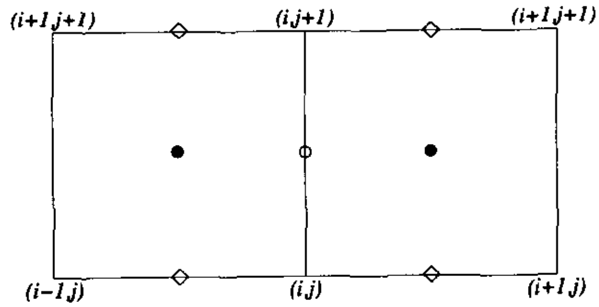

FIG. 4. Interior X stencil: ○, WX and KXX; ◇, WY and KYY; ●, KXY.

where $i = 2, ..., N - 1$, $j = 1, ..., M - 1$, and the Y component of $\mathcal{K}\vec{A}$ is defined by

$$\begin{aligned}
(\mathcal{K}\vec{A})^Y_{(i,j)} &= \tfrac{1}{2}KXY_{(i+1/2,j+1/2)}AX_{(i+1/2,j)} \\
&\quad + \tfrac{1}{2}KXY_{(i+1/2,j-1/2)}AX_{(i+1/2,j-1)} \\
&\quad + KYY_{(i+1/2,j)}AY_{(i,j)}, \\
(\mathcal{K}\vec{A})^Y_{i,1} &= KXY_{(i,3/2)}AX_{(i+1/2,1)} \\
&\quad + KYY_{(i+1/2,1)}AY_{(i,1)}, \\
(\mathcal{K}\vec{A})^Y_{(i,M)} &= KXY_{(i+1/2,M-1/2)}AX_{(i+1/2,M-1)} \\
&\quad + KYY_{(i+1/2,M)}AY_{(i,M)},
\end{aligned} \tag{44}$$

where $i = 1, ..., N - 1$, $j = 2, ..., M - 1$. The operator $\mathcal{D}$ is zero except for

$$\begin{aligned}
(\mathcal{D}U)_{(0,j)} &= \alpha_{(0,j)}U_{(0,j)}, \\
(\mathcal{D}U)_{(N,j)} &= \alpha_{(N,j)}U_{(N,j)}, \\
(\mathcal{D}U)_{(i,0)} &= \alpha_{(i,0)}U_{(i,0)}, \\
(\mathcal{D}U)_{(i,M)} &= \alpha_{(i,M)}U_{(i,M)}.
\end{aligned}$$

(See Fig. 1.)

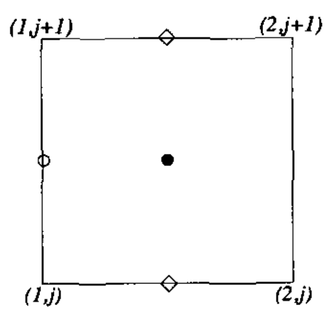

FIG. 5. Left boundary stencil, symbols are as in Fig. 4.

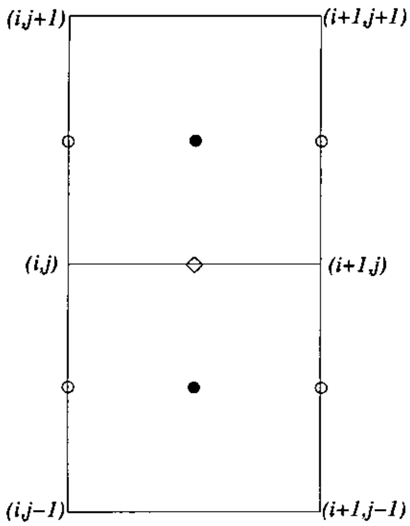

FIG. 6. Interior Y stencil, symbols as in Fig. 4.

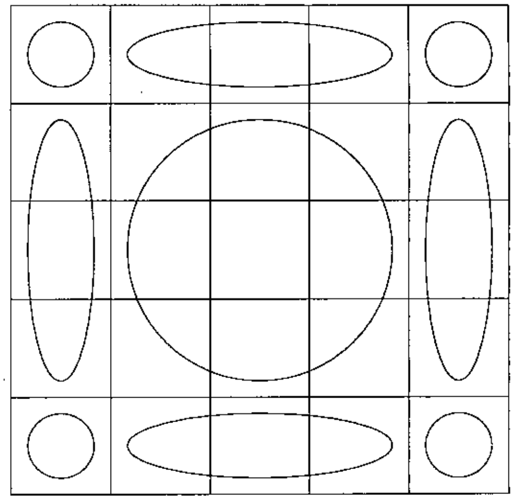

FIG. 7. Domains of uniformity.

3.6. *The Elliptic Operator*

The operator form of the finite-difference scheme for the elliptic boundary-value problem (1) and (2) is

$$\mathcal{A}U = (\mathcal{B}\mathcal{K}\mathcal{C} + \mathcal{D})U = F. \tag{45}$$

It is convenient to give the explicit form of the difference equation for approximating the elliptic equation $-\mathbf{div}\ \mathbf{K}\ \mathbf{grad}\ u = f$ using the flux $\vec{W} = -K\ \mathbf{GRAD}\ U$ as the discrete cell conservation law

$$\frac{WX_{(i+1,j)} - WX_{(i,j)}}{hX} + \frac{WY_{(i,j+1)} - WY_{(i,j)}}{hY} = F_{(i,j)}. \tag{46}$$

Because the expressions for multiplication by K and for **GRAD** U have several cases, there are nine different cases for the formula for $\mathcal{A}U$; each case is called a domain of uniformity (see Fig. 7). Only three typical cases are described:

internal cells: $i = 2, ..., N-2; j = 2, ..., M-2,$

near boundary cells: $i = 1; j = 2, ..., M-2$

corner cells: $i = 1; j = 1.$

The result for the internal cells is (see Fig. 8)

$$\begin{aligned}
&-KXX_{(i+1,j+1/2)}\frac{U_{(i+1,j)} - U_{(i,j)}}{hX^2} \\
&-KXY_{(i+3/2,j+1/2)}\frac{U_{(i+1,j+1)} - U_{(i+1,j-1)}}{4hXhY} \\
&+KXX_{(i,j+1/2)}\frac{U_{(i,j)} - U_{(i-1,j)}}{hX^2} \\
&+KXY_{(i-1/2,j+1/2)}\frac{U_{(i-1,j+1)} - U_{(i-1,j-1)}}{4hXhY} \\
&-KXY_{(i+1/2,j+3/2)}\frac{U_{(i+1,j+1)} - U_{(i-1,j+1)}}{4hXhY} \\
&-KYY_{(i+1/2,j+1)}\frac{U_{(i,j+1)} - U_{(i,j)}}{hY^2} \\
&+KXY_{(i+1/2,j-1/2)}\frac{U_{(i+1,j-1)} - U_{(i-1,j-1)}}{4hXhY} \\
&+KYY_{(i+1/2,j)}\frac{U_{(i,j)} - U_{(i,j-1)}}{hY^2} = F_{(i,j)}.
\end{aligned} \tag{47}$$

The result for cells near the west boundary is (see Fig. 9)

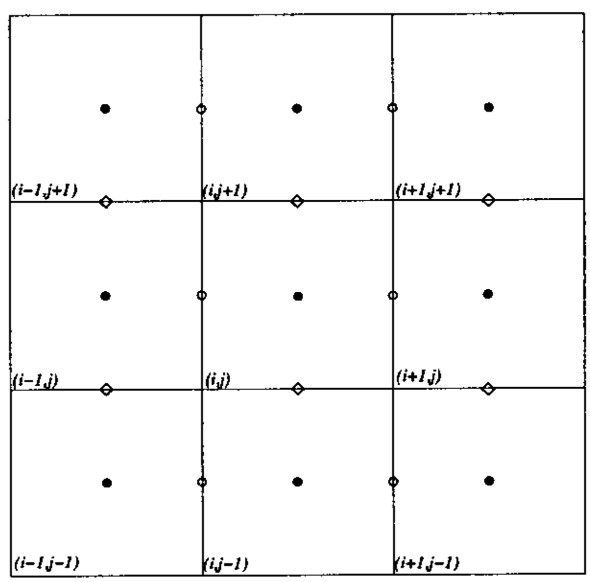

FIG. 8. Interior elliptic stencil: ○, WX; ◇, WY; ●, U.

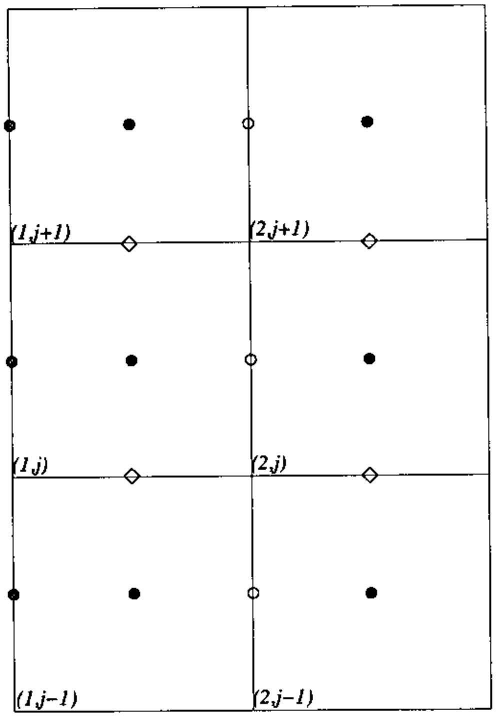

FIG. 9. Left near-boundary elliptic stencil: ●, U; ⊗, boundary U and WS; ○, WX; ◇, WX.

$$
\begin{aligned}
&-KXX_{(2,j+1/2)} \frac{U_{(2,j)} - U_{(1,j)}}{hX^2} \\
&-KXY_{(5/2,j+1/2)} \frac{U_{(2,j+1)} - U_{(2,j-1)}}{4hXhY} \\
&+KXX_{(1,j+1/2)} \frac{U_{(1,j)} - U_{(0,j)}}{hX^2/2} \\
&+KXY_{(3/2,j+1/2)} \frac{U_{(1,j+1)} - U_{(1,j-1)}}{4hXhY} \\
&-KXY_{(3/2,j+3/2)} \frac{1}{4}\left(\frac{U_{(1,j+1)} - U_{(0,j+1)}}{hX/2hY} + \frac{U_{(2,j+1)} - U_{(1,j+1)}}{hXhY}\right) \\
&-KYY_{(3/2,j+1)} \frac{U_{(1,j+1)} - U_{(1,j)}}{hY^2} \\
&+KXY_{(3/2,j-1/2)} \frac{1}{4}\left(\frac{U_{(1,j-1)} - U_{(0,j-1)}}{hX/2hY} + \frac{U_{(2,j-1)} - U_{(1,j-1)}}{hXhY}\right) \\
&+KYY_{(3/2,j)} \frac{U_{(1,j)} - U_{(1,j-1)}}{hY^2} = F_{(1,j)}.
\end{aligned} \tag{48}
$$

The result for a cell in the southwest corner is (see Fig. 10)

$$
\begin{aligned}
&-KXX_{(2,3/2)} \frac{U_{(2,1)} - U_{(1,1)}}{hX^2} \\
&-KXY_{(5/2,3/2)} \frac{1}{4}\left(\frac{U_{(2,1)} - U_{2,0)}}{hXhY/2} + \frac{U_{(2,2)} - U_{(2,1)}}{hXhY}\right) \\
&+KXX_{(1,3/2)} \frac{U_{(1,1)} - U_{(0,1)}}{hX^2/2} \\
&+KXY_{(3/2,3/2)} \frac{1}{4}\left(\frac{U_{(1,1)} - U_{(1,0)}}{hY/2hX} + \frac{U_{(1,2)} - U_{(1,1)}}{hXhY}\right) \\
&-KXY_{(3/2,5/2)} \frac{1}{4}\left(\frac{U_{(1,2)} - U_{(0,2)}}{hX/2hY} + \frac{U_{(2,2)} - U_{(1,2)}}{hXhY}\right) \\
&-KYY_{(3/2,2)} \frac{U_{(1,2)} - U_{(1,1)}}{hY^2} \\
&+KXY_{(3/2,3/2)} \frac{1}{4}\left(\frac{U_{(1,1)} - U_{(0,1)}}{hX/2hY} + \frac{U_{(2,1)} - U_{(1,1)}}{hXhY}\right) \\
&+KYY_{(3/2,1)} \frac{U_{(1,1)} - U_{(1,0)}}{hY^2/2} = F_{(1,1)}.
\end{aligned} \tag{49}
$$

Next consider the approximation of the boundary conditions for which two typical cases are described:

west boundary: $i = 0; j = 2, ..., M - 2$,

southwest corner: $i = 0; j = 1$.

The result for internal cells on the west boundary is (see Fig. 11)

$$-(\mathcal{K}\ \mathbf{GRAD}\ U)_{(0,j)} + \Upsilon_{(0,j)} U_{(0,j)} = \Psi_{(0,j)}, \tag{50}$$

or

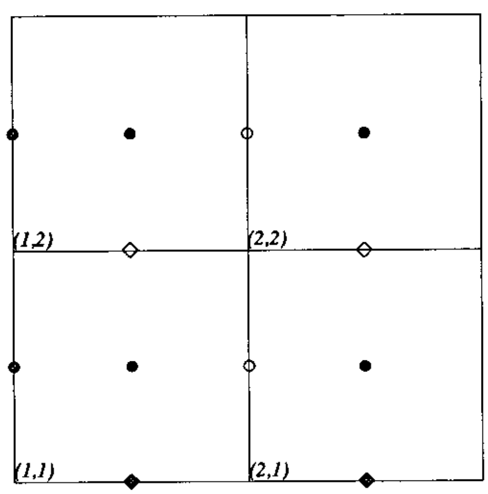

FIG. 10. Corner elliptic stencil: symbols as in Fig. 9, and ⊗, boundary U and WY.

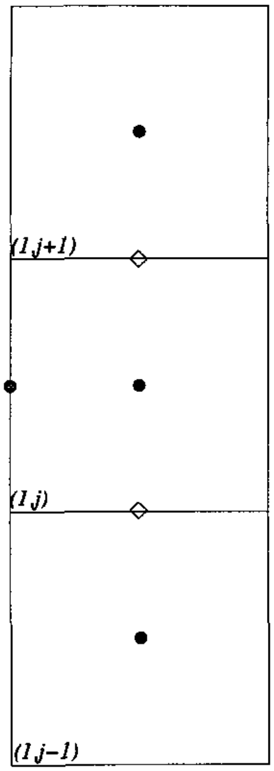

FIG. 11. Left boundary stencil: symbol, as in Fig. 9.

$$-KXX_{(1,j+1/2)}\frac{U_{(1,j)}-U_{(0,j)}}{hX/2}$$
$$-KXY_{(3/2,j+1/2)}\frac{1}{2}\left(\frac{U_{(1,j)}-U_{(1,j-1)}}{hY}+\frac{U_{(1,j+1)}-U_{(1,j)}}{hY}\right) \qquad (51)$$
$$+\Upsilon_{(0,j)}U_{(0,j)}=\Psi_{(0,j)}.$$

The result for the point on west boundary near the south-west corner is (see Fig. 12)

$$-(\mathcal{K}\ \mathbf{GRAD}\ U)_{(0,1)}+\alpha_{(0,1)}U_{(0,1)}=\psi_{(0,1)} \qquad (52)$$

or

$$-KXX_{(1,3/2)}\frac{U_{(1,1)}-U_{(0,1)}}{hX/2}$$
$$-KXY_{(3/2,3/2)}\frac{1}{2}\left(\frac{U_{(1,1)}-U_{(1,0)}}{hY/2}+\frac{U_{(1,2)}-U_{(1,1)}}{hY}\right) \qquad (53)$$
$$+\alpha_{(0,1)}U_{(0,1)}=\psi_{(0,1)}.$$

3.7. *The Matrix Problem*

From the formula (45), $\mathcal{A}=\mathcal{B}\mathcal{K}\mathcal{C}+\mathcal{D}$, and $\mathcal{B}=\mathcal{C}^*$, $\mathcal{K}=\mathcal{K}^*$, $\mathcal{K}>0$, $\mathcal{D}=\mathcal{D}^*$, and $\mathcal{D}\geq 0$, it is clear that the operator $\mathcal{A}$ is symmetric and positive. The note at the end of Section 3.4 and the argument given for (32) can be generalized to show that if $\mathcal{A}U=0$ and Υ is positive at one point of the boundary, then $U=0$, and then that $\mathcal{A}$ is positive definite. To do this, first note that if $\mathcal{A}U=0$, then the positive definiteness of $\mathcal{K}$ implies that $\mathcal{C}U=0$. The fact that the first component of **GRAD** $U=0$ implies that U is constant along vertical lines, while the second component being zero implies that U is constant along horizontal lines, so that U is then a constant. The boundary condition gives $U=0$. This then implies that the matrix of the finite-difference approximation to the elliptic problem, when multiplied by a diagonal matrix of the volumes that appear in the discrete scalar inner product, has the same properties as the operator $\mathcal{A}$. The stencil for the elliptic operator $\mathcal{A}$ is nearest neighbor, which implies that the matrix of $\mathcal{A}$ has nine non-zero bands. The explicit form for $\mathcal{A}$ is neither useful nor illuminating, so it is not written out.

4. SUPPORT OPERATORS ON GENERAL GRIDS

In this section, the ideas in Section 3 on support operators on rectangular grids are extended to general logically rectangular grids. Because rectangular and logically rectangular grids have the same *logical* structure, much of the notation is the same for both problems. However, in the case of general grids, the description of vector fields is significantly more complicated. Only the case of diagonal **K** is presented to reduce the length of the presentation. A particularly important point is to understand why the discrete gradient is no longer local.

4.1. *Discretization in Logically Rectangular Grids*

A logically rectangular grid can be indexed in exactly the same way as a rectangular grid (see Fig. 13). Thus the nodes of the grid are labeled using (i, j), $1\leq i\leq N$, $1\leq j\leq M$,

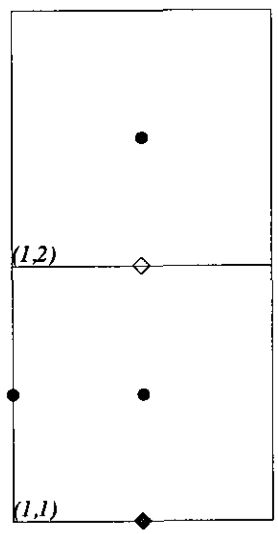

FIG. 12. Left near-boundary near S-W corner stencil: symbols as in Fig. 10.

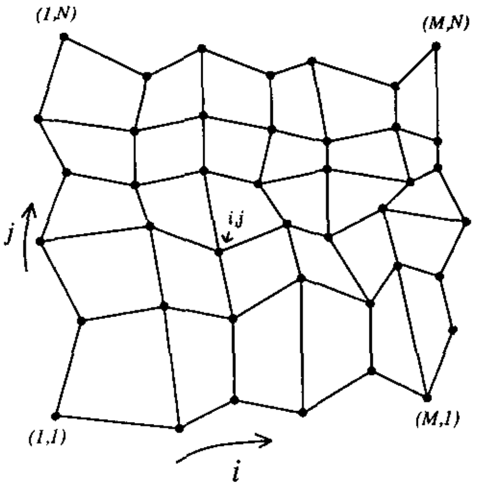

FIG. 13. Logically rectangular grid.

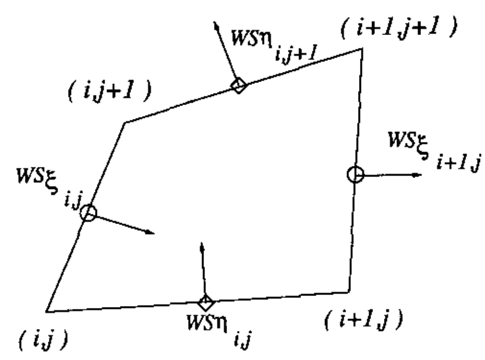

FIG. 15. Discretization of a vector.

and the quadrilateral defined by the points (i, j), $(i + 1, j)$, $(i + 1, j + 1)$, and $(i, j + 1)$ is called the (i, j) cell (see Fig. 14). The area of this cell is denoted by $VC_{(i,j)}$. The length of the side of the (i, j) cell that connects the vertices (i, j) and $(i, j + 1)$ is denoted $S\xi_{(i,j)}$, while the length of the side that connects the vertices (i, j) and $(i + 1, j)$ is denoted $S\eta_{(i,j)}$. The angle between any two adjacent sides of cell (i, j) that meet at node (k, l) is denoted $\varphi^{(i,j)}_{k,l}$ (the angle $\varphi^{(i,j)}_{(i+1,j)}$ is displayed in Fig. 14).

It is usual to place some mild smoothness assumptions on the grid. We assume that there exist constants $C^{(1)}_{\max}$ and $C^{(1)}_{\min}$ which do not depend on h, so that

$$C^1_{\min} h^2 \leq VC_{(i,j)} \leq C^1_{\max} h^2, \tag{54}$$

and that there exist constants $C^{(2)}_{\max}$ and $C^{(2)}_{\min}$ which do not depend on h, that

$$C^2_{\min} h \leq S\xi_{(i,j)}, S\eta_{(i,j)} \leq C^2_{\max} h, \tag{55}$$

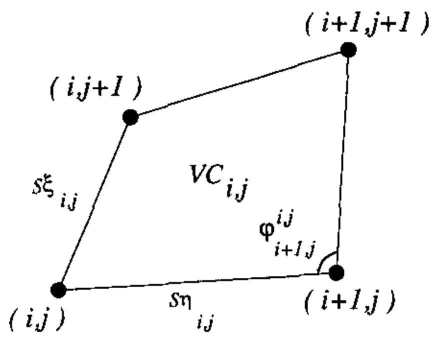

FIG. 14. Typical cell of logically rectangular grid.

and that there exists a constant $\delta > 0$ such that

$$\sin(\varphi^{(i,j)}_{(k,l)}) > \delta, \tag{56}$$

where δ is a constant which does not depend on h. Under these conditions, the support-operator discretization is second-order accurate, as it is in a simple rectangular grid.

The notation for discrete scalar functions is the same as in the case of a rectangular grid and thus $U_{(i,j)}$ denotes a cell value. Also, for discretizing the boundary conditions, values of scalar functions on the boundary segments are used (see Subsection 3.1). Vector functions are described using their components which are the orthogonal projections in the direction which is perpendicular to the sides of the cell (see Fig. 15). To distinguish this from the case of a rectangular grid where these projections coincide with the Cartesian components of the vector, the notation $WS\xi_{(i,j)}$ is used for the component at the center of the side $S\xi_{(i,j)}$, and $WS\eta_{(i,j)}$ is used for the component at the center of the side $S\eta_{(i,j)}$.

4.2. *Spaces of Discrete Functions*

The space of discrete scalar functions is labeled HC as in the case of a rectangular grid and has the inner product

$$\begin{aligned}(U, V)_{HC} = &\sum_{i=1}^{N-1}\sum_{j=1}^{M-1} U_{(i,j)}V_{(i,j)}VC_{(i,j)} \\ &+ \sum_{i=1}^{N-1} U_{(i,1)}V_{(i,1)}S\eta_{(i,1)} + \sum_{j=1}^{M-1} U_{(N,j)}V_{(N,j)}S\xi_{(N,j)} \\ &+ \sum_{i=1}^{N-1} U_{(i,M)}V_{(i,M)}S\eta_{(i,M)} \sum_{j=1}^{M-1} U_{(1,j)}V_{(1,j)}S\xi_{(1,j)}.\end{aligned} \tag{57}$$

The space of vector functions is labeled $\mathcal{HS}$ and has the inner product

$$(\vec{A}, \vec{B})_{\mathcal{HS}} = \sum_{i=1}^{N-1}\sum_{j=1}^{M-1} (\vec{A}, \vec{B})_{(i,j)} VC_{(i,j)}, \tag{58}$$

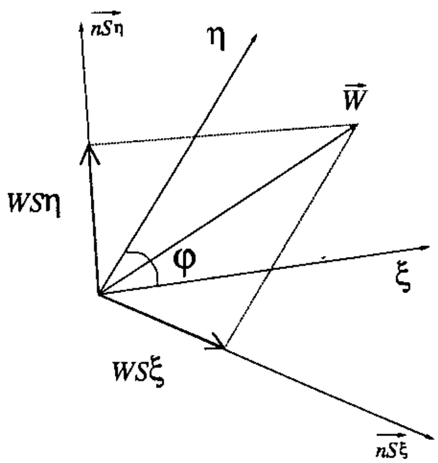

FIG. 16. Components of vector in local basis.

where $(\vec{A}, \vec{B})$ is the dot product of two vectors. A formula for this dot product in terms of the components of the vectors perpendicular to the cell sides is needed (see Fig. 16). Thus suppose that the axes ξ and η form a non-orthogonal basis system and that φ is the angle between these axes. If the unit normals to the axes are $\vec{nS}\,\xi$ and $\vec{nS}\,\eta$, then the components of the vector $\vec{W}$ in this basis are the orthogonal projections $WS\xi$ and $WS\eta$ of $\vec{W}$ onto the normal vectors. See the discussion in Chap. 2 of Knupp and Steinberg [6] for more details. Some simple vector algebra shows that if $\vec{A} = (AS\xi, AS\eta)$ and $\vec{B} = (BS\xi, BS\eta)$ then the expression for the dot product is

$$(\vec{A}, \vec{B}) = \frac{AS\xi BS\xi + AS\eta BS\eta + (AS\xi BS\eta + AS\eta BS\xi)\cos(\varphi)}{\sin^2(\varphi)}. \tag{59}$$

Now the previous formula is used to obtain an analog of the formula used in the rectangular grid case:

$$\begin{aligned}(\vec{A}, \vec{B})_{(i,j)} = \sum_{k,l=0}^{1} \frac{V^{(i,j)}_{(i+k,j+l)}}{\sin^2(\varphi^{(i,j)}_{(i+k,j+l)})} &[AS\xi_{(i+k,j)}BS\xi_{(i+k,j)} + AS\eta_{(i,j+l)}BS\eta_{(i,j+l)} \\ &+ (-1)^{k+l}(AS\xi_{(i+k,j)}BS\eta_{(i,j+l)} \\ &+ AS\eta_{(i,j+l)}BS\xi_{(i+k,j)})\cos(\varphi^{(i,j)}_{(i+k,j+l)})],\end{aligned} \tag{60}$$

where the $V^{(i,j)}_{(i+k,j+l)}$ are some weights for which

$$\sum_{k,l=0}^{1} V^{(i,j)}_{(i+k,j+l)} = VC_{(i,j)}. \tag{61}$$

In this formula each index (k, l) corresponds to one of the vertices of the (i, j) cell. In practice, the volumes that are summed in Formula (60) are taken to be one half of the area of the triangle in the (i, j) cell which contains an angle at the node $(i + k, j + l)$.

For the computation of adjoint relationships it is helpful to introduce the *formal* inner products, $[\cdot, \cdot]$, in the spaces of scalar and vector functions. In HC

$$\begin{aligned}[U, V]_{HC} = &\sum_{i=1}^{N-1}\sum_{j=1}^{M-1} U_{(i,j)}V_{(i,j)} + \sum_{i=1}^{N-1} U_{(i,1)}V_{(i,1)} \\ &+ \sum_{j=1}^{M-1} U_{(N,j)}V_{(N,j)} + \sum_{i=1}^{N-1} U_{(i,M)}V_{(i,M)} + \sum_{j=1}^{M-1} U_{(1,j)}V_{(1,j)},\end{aligned} \tag{62}$$

and in $\mathcal{HS}$

$$[\vec{A}, \vec{B}]_{\mathcal{HS}} \sum_{i=1}^{N}\sum_{j=1}^{M-1} AS\xi_{(i,j)}BS\xi_{(i,j)} + \sum_{i=1}^{N-1}\sum_{j=1}^{M} AS\eta_{(i,j)}BS\eta_{(i,j)}. \tag{63}$$

Then the relationships between the natural inner product and the formal inner products are

$$(U, V)_{HC} = [\mathcal{M}U, V]_{HC}, \qquad (\vec{A}, \vec{B})_{\mathcal{HS}} = [\mathcal{S}\vec{A}, \vec{B}]_{\mathcal{HS}}, \tag{64}$$

where $\mathcal{M}$ is the symmetric positive operator in the formal inner product, that is,

$$[\mathcal{M}U, V]_{HC} = [U, \mathcal{M}V]_{HC}, \qquad [\mathcal{M}U, U]_{HC} > 0. \tag{65}$$

A comparison of the natural and formal inner products gives

$$(\mathcal{M}U)_{(i,j)} = VC_{(i,j)}U_{(i,j)}, \quad i = 1, ..., N-1; j = 1, ..., M-1, \tag{66}$$

$$(\mathcal{M}U)_{(i,j)} = S\xi_{(i,j)}U_{(i,j)}, \quad i = 1 \text{ and } i = N; j = 1, ..., M-1; \tag{67}$$

$$(\mathcal{M}U)_{(i,j)} = S\eta_{(i,j)}U_{(i,j)}, \quad i = 1, ..., N-1; j = 1 \text{ and } j = M. \tag{68}$$

The operator $\mathcal{S}$ can be written in block form:

$$\mathcal{S}\vec{A} = \begin{pmatrix} S_{11} & S_{12} \\ S_{21} & S_{22} \end{pmatrix}\begin{pmatrix} AS\xi \\ AS\eta \end{pmatrix} = \begin{pmatrix} S_{11}AS\xi + S_{12}AS\eta \\ S_{21}AS\xi + S_{22}AS\eta \end{pmatrix}. \tag{69}$$

This operator is symmetric and positive in the formal inner product:

$$[\mathcal{S}\vec{A}, \vec{B}]_{\mathcal{HS}} = [\vec{A}, \mathcal{S}\vec{B}]_{\mathcal{HS}}, \qquad [\mathcal{S}\vec{A}, \vec{A}]_{\mathcal{HS}} > 0. \tag{70}$$

A comparison of formal and natural inner products gives

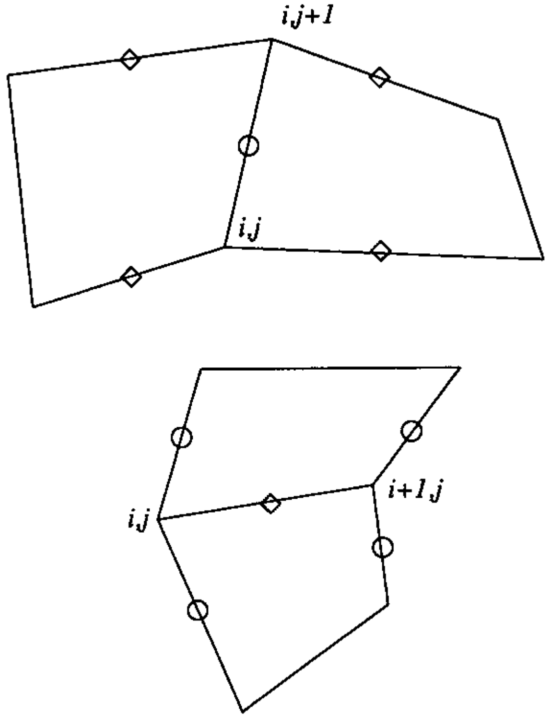

FIG. 17. Stencils for operators S_{12} (top) and S_{21} (bottom).

$$(\vec{A},\vec{B})_{\mathcal{HS}} = [\mathcal{S}\vec{A},\vec{B}]_{\mathcal{HS}} = \sum_{i=1}^{N}\sum_{j=1}^{M-1} [(S_{11}AS\xi)_{(i,j)} + (S_{12}AS\eta)_{(i,j)}]BS\xi_{(i,j)} + \sum_{i=1}^{N-1}\sum_{j=1}^{M} [(S_{21}AS\xi)_{(i,j)} + (S_{22}AS\eta)_{(i,j)}]BS\eta_{(i,j)}, \tag{71}$$

from which formulas for operator $\mathcal{S}$ can be derived:

$$(S_{11}AS\xi)_{(i,j)} = \left(\sum_{k,l=0}^{1} \frac{V_{(i,j+l)}^{(i-k,j)}}{\sin^2(\varphi_{(i,j+l)}^{(i-k,j)})}\right) AS\xi_{(i,j)},$$

$$(S_{12}AS\eta)_{(i,j)} = \sum_{k,l=0}^{1} (-1)^{k+l} \frac{V_{(i,j+l)}^{(i-k,j)}}{\sin^2(\varphi_{(i,j+l)}^{(i-k,j)})} \cos(\varphi_{(i,j+l)}^{(i-k,j)}) AS\eta_{(i-k,j+l)},$$

$$(S_{21}AS\eta)_{(i,j)} = \sum_{k,l=0}^{1} (-1)^{k+l} \frac{V_{(i+l,j)}^{(i,j-k)}}{\sin^2(\varphi_{(i+l,j)}^{(i,j-k)})} \cos(\varphi_{(i+l,j)}^{(i,j-k)}) AS\eta_{(i+l,j-k)},$$

$$(S_{22}AS\eta)_{(i,j)} = \left(\sum_{k,l=0}^{1} \frac{V_{(i+l,j)}^{(i,j-k)}}{\sin^2(\varphi_{(i+l,j)}^{(i,j-k)})}\right) AS\eta_{(i,j)}. \tag{72}$$

Actually, these formulas are valid only for $i = 2, ..., N-2$; $j = 2, ..., M-2$, but it is possible to prove that if fictitious cells with zero volumes are introduced then these formulas are valid for all i and j. The operators S_{11} and S_{22} are diagonal and the stencils for the operators S_{12} and S_{21} are shown in Fig. 17.

4.3. *The Prime Operator*

In the interior of the region, the prime operator $\mathcal{B}$, which is the analog of the divergence, is given by

$$(\mathcal{B}\vec{W})_{(i,j)} = (\mathbf{DIV}\,\vec{W})_{(i,j)} = \frac{1}{VC_{(i,j)}}\{(WS\xi_{(i+1,j)}S\xi_{(i+1,j)} - WS\xi_{(i,j)}S\xi_{(i,j)}) + (WS\eta_{(i,j+1)}S\eta_{(i,j+1)} - WS\eta_{(i,j+1)}S\eta_{(i,j+1)})\}, \tag{73}$$

while on the boundary it is (here the operator B is an approximation of the normal component of vector)

$$\begin{aligned} (\mathcal{B}\vec{W})_{(i,0)} &= -WS\eta_{(i,1)}, & i &= 1, ..., N-1,\\ (\mathcal{B}\vec{W})_{(i,M)} &= +WS\eta_{(i,M)}, & i &= 1, ..., N-1,\\ (\mathcal{B}\vec{W})_{(0,j)} &= -WS\xi_{(1,j)}, & j &= 1, ..., M-1,\\ (\mathcal{B}\vec{W})_{(N,j)} &= +WS\xi_{(N,j)}, & j &= 1, ..., M-1. \end{aligned} \tag{74}$$

4.4. *The Derived Operator*

The derived operator, which is the analog of the gradient, is defined by $\mathcal{C} = \mathcal{B}^*$ where the adjoint is taken in the natural inner products. For a general non-orthogonal logically rectangular grid, it is not possible to write simple explicit formulas for the components of the operator $\mathcal{C}$, but it is possible to find a formula for $\mathcal{C}$ in terms of $\mathcal{M}$, $\mathcal{S}$, and $\mathcal{B}$.

Recall that $\mathcal{B}: \mathcal{HS} \to HC$. The definition of the adjoint gives

$$(\mathcal{B}\vec{W}, U)_{HC} = (\vec{W}, \mathcal{B}^*U)_{\mathcal{HS}}, \tag{75}$$

which can be translated to the formal inner products as

$$[\mathcal{B}\vec{W}, \mathcal{M}U]_{HC} = [\vec{W}, \mathcal{S}\mathcal{B}^*U]_{\mathcal{HS}}. \tag{76}$$

The formal adjoint $\mathcal{B}^{\otimes}$ of $\mathcal{B}$ is defined to be the adjoint in the formal inner product, which gives

$$[\vec{W}, \mathcal{B}^{\otimes}\mathcal{M}U]_{\mathcal{HS}} = [\vec{W}, \mathcal{S}\mathcal{B}^*U]_{\mathcal{HS}}. \tag{77}$$

This relationship must be true for all $\vec{W}$ and U, so

$$\mathcal{B}^{\otimes}\mathcal{M} = \mathcal{S}\mathcal{B}^* \tag{78}$$

or

$$\mathcal{B}^* = \mathcal{S}^{-1}\mathcal{B}^{\otimes}\mathcal{M}. \tag{79}$$

Thus the discrete gradient is given by

$$\mathbf{GRAD} = -\mathcal{C} = -\mathcal{S}^{-1}\mathcal{B}^{\otimes}\mathcal{M}. \tag{80}$$

Note that $\mathcal{S}$ is banded and consequently $\mathcal{S}^{-1}$ is not banded and then **GRAD** is not banded, that is, **GRAD** has a *non-local* stencil, and consequently the matrix for **GRAD** is full. In fact, this is not a catastrophic problem. At the end of this section we show how to compute with such operators. There is an explicit formula for $\mathcal{B}^{\otimes}$:

$$-((\mathcal{B}^{\otimes}\mathcal{M})U)_{(i,j)} = \begin{pmatrix} S\xi_{(i,j)}(U_{(i,j)} - U_{i-1,j}) \\ S\eta_{(i,j)}(U_{(i,j)} - U_{i,j-1}) \end{pmatrix}. \quad (81)$$

In the case of a rectangular grid, the formulas in this section reduce to the formulas in Section 3. Moreover, for an orthogonal grid, the operator $\mathcal{S}$ is diagonal and therefore a simple explicit expression can be given for **GRAD**. It is also important to note that the expressions for all of the operators contain only coordinate invariant quantities like volumes, areas, and angles, so that the description of scalar and vector functions is also coordinate system invariant. This means that the constructed operators can be used in any coordinate system by simply changing the formulas for geometrical quantities.

4.5. *The Elliptic Operator*

The support-operator approximation for the PDE (1) is defined to be

$$(\mathbf{DIV}\ \mathcal{K}\ \mathbf{GRAD}\ U)_{(i,j)} = F_{(i,j)} \quad (82)$$

for the interior nodes, while on the boundary the expressions coincide with those on a rectangular grid. For example, for $i = 0$,

$$-(\mathcal{K}\ \mathbf{GRAD}\ U)_{(0,j)} + \Upsilon_{(0,j)}U_{(0,j)} = \Psi_{(0,j)}. \quad (83)$$

Again, note that this approximation has a nonlocal stencil. Also, Υ and Ψ must be computed at a point in the boundary segment of the cell.

4.6. *Solving Problems with Non-local Stencils*

In this section, an outline of a solution procedure for the system (82) and (83) is given. For simplicity, assume that $K = I$, the identity matrix, and that the boundary condition is the homogeneous Dirichlet condition, so that **GRAD** $= -$**DIV***. The solution of elliptic problem (82) is obtained as the steady-state solution of the heat equation. An implicit finite-difference scheme for this heat equation is

$$\frac{U^{n+1} - U^n}{\Delta t} - \mathbf{DIV}\ \mathcal{K}\ \mathbf{GRAD}\ U^{n+1} = f, \quad (84)$$

where upper indices involving n correspond to time levels. As before, the flux is given by

$$\vec{W} = -\mathbf{GRAD}\ U \quad (85)$$

and then the heat equation (84) can be written in flux form

$$\frac{U^{n+1} - U^n}{\Delta t} + \mathbf{DIV}\ \vec{W}^{n+1} = f \quad (86)$$

$$\vec{W}^{n+1} = -\mathbf{GRAD}\ U^{n+1} = \mathcal{S}^{-1}\,\mathbf{DIV}^{\otimes}\,\mathcal{M}U^{n+1}. \quad (87)$$

The first equation can be solved for U^{n+1} and then this result can be substituted into the second equation to get

$$\vec{W}^{n+1} = -\Delta t\,\mathcal{S}^{-1}\,\mathbf{DIV}^{\otimes}\,\mathcal{M}\,\mathbf{DIV}\ \vec{W}^{n+1} + F, \quad (88)$$

where F contains known quantities. Applying the operator $\mathcal{S}$ to this equation gives

$$\mathcal{S}\vec{W}^{n+1} = -\Delta t\,\mathbf{DIV}^{\otimes}\,\mathcal{M}\,\mathbf{DIV}\ \vec{W}^{n+1} + \mathcal{S}F \quad (89)$$

or

$$(\mathcal{S} + \Delta t\,\mathbf{DIV}^{\otimes}\,\mathcal{M}\,\mathbf{DIV})\vec{W}^{n+1} = \mathcal{S}F, \quad (90)$$

which gives an equation for determining the fluxes at the new time level. It is possible to show that the matrix for this system is symmetric and positive definite, so that efficient iteration methods can be used to solve this system. After the flux $\vec{W}^{n+1}$ is computed, U^{n+1} is computed explicitly from the first equation in (84).

5. THE MAPPING METHOD

When the boundary-value problem (1) and (2) is given in a non-rectangular region that can be mapped to a rectangular region, then the mapping method can be used to transform the boundary-value problem that has exactly the same form as the original, and consequently the support-operator method for a rectangular region can be applied to the transformed problem. This discussion of combining the mapping and the support-operators method follows the discussion in Knupp and Steinberg [6].

In this approach, it is assumed that the grid is given by an analytic transformation,

$$x = x(\xi, \eta), \qquad y = y(\xi, \eta), \quad (91)$$

of logical space (ξ, η), $0 \le \xi, \eta \le 1$, to physical space (x, y). The uniform grid,

$$\xi_i = \frac{i}{M-1}, \qquad \eta_j = \frac{j}{N-1}, \quad (92)$$

is the chosen logical space, and then the grid in physical space is given by

$$x_{i,j} = x(\xi_i, \eta_j), \qquad y_{i,j} = y(\xi_i, \eta_j). \tag{93}$$

The boundary of the physical region is given by the image of the boundary of the logical region, that is, the grid is boundary conforming.

Next, the PDE (1) and the BC (2) are transformed to logical space. To do this, let the Jacobian matrix of the transformation be given by

$$J = \begin{pmatrix} x_\xi & y_\xi \\ x_\eta & y_\eta \end{pmatrix}, \tag{94}$$

and then the Jacobian $\mathbf{J}$ is given by the determinant of the Jacobian matrix

$$\mathbf{J} = x_\xi y_\xi - x_\eta y_\eta. \tag{95}$$

It is always assumed that $\mathbf{J} > 0$. Next introduce the cofactor matrix

$$C = \mathbf{J} J^{-1} = \begin{pmatrix} y_\eta & -y_\xi \\ -x_\eta & x_\xi \end{pmatrix}. \tag{96}$$

If column vectors are used, then the chain rule gives

$$\mathbf{grad}_{x,y} u = \frac{1}{\mathbf{J}} C \, \mathbf{grad}_{\xi,\eta} u = \mathcal{J}^{-1} \, \mathbf{grad}_{\xi,\eta} u, \tag{97}$$

and then the product rule for derivatives gives

$$\mathbf{div}_{x,y} \vec{A} = \frac{1}{\mathbf{J}} \mathbf{div}_{\xi,\eta} (C^* \vec{A}). \tag{98}$$

Consequently, the PDE (1.1),

$$-\mathbf{div}_{x,y} K \, \mathbf{grad}_{x,y} u = f, \tag{99}$$

is transformed to

$$-\frac{1}{\mathbf{J}} \mathbf{div}_{\xi,\eta} \tilde{K} \, \mathbf{grad}_{\xi,\eta} u = f, \tag{100}$$

or

$$-\mathbf{div}_{\xi,\eta} \tilde{K} \, \mathbf{grad}_{\xi,\eta} u = \tilde{f}, \tag{101}$$

where

$$\tilde{u}(\xi, \eta) = u(x(\xi, \eta), y(\xi, \eta)),$$

$$\tilde{K}(\xi, \eta) = \frac{1}{\mathbf{J}(\xi, \eta)} C^*(\xi, \eta) \, K(x(\xi, \eta), y(\xi, \eta)) C(\xi, \eta), \tag{102}$$

$$\tilde{f}(\xi, \eta) = \mathbf{J}(\xi, \eta) f(x(\xi, \eta), y(\xi, \eta)).$$

Note that $\tilde{K}$ is symmetric and positive definite if K is.

The specific formulas are

$$\tilde{K}_{\xi\xi} = +\frac{1}{\mathbf{J}} (+K_{xx} y_\eta^2 - 2 \, K_{xy} x_\eta y_\eta + K_{yy} x_\eta^2), \tag{103}$$

$$\tilde{K}_{\xi\eta} = -\frac{1}{\mathbf{J}} (+K_{xx} y_\xi y_\eta - K_{xy} (x_\xi y_\eta + x_\eta y_\xi) + K_{yy} x_\xi x_\eta), \tag{104}$$

$$\tilde{K}_{\eta\eta} = +\frac{1}{\mathbf{J}} (+K_{xx} y_\xi^2 - 2 \, K_{xy} x_\xi y_\xi + K_{yy} x_\xi^2). \tag{105}$$

To transform the boundary condition to logical coordinates, first note that the boundary of the physical region is given by the four curves

$$\begin{aligned} &(x(\xi, 0), y(\xi, 0)), \ (x(\xi, 1), y(\xi, 1)), \qquad 0 \le \xi \le 1, \\ &(x(0, \eta), y(0, \eta)), (x(1, \eta), y(1, \eta)), \qquad 0 \le \eta \le 1. \end{aligned} \tag{106}$$

In terms of the inverse transformation, the boundary curves are given by

$$\xi(x, y) = C, \qquad \eta(x, y) = C, \qquad C = \{0, 1\}. \tag{107}$$

These curves, respectively, have

$$\vec{N}_1 = \mathbf{grad}_{x,y} \xi, \quad \vec{N}_2 = \mathbf{grad}_{x,y} \eta \tag{108}$$

as normal vectors and then the unit normals are

$$\vec{n}_1 = \frac{\vec{N}_1}{|\vec{N}_1|}, \qquad \vec{n}_2 = \frac{\vec{N}_2}{|\vec{N}_2|}. \tag{109}$$

To write everything in terms of logical coordinates, note that

$$|\vec{N}_1|^2 = \frac{x_\xi^2 + y_\xi^2}{\mathbf{J}}, \qquad |\vec{N}_2|^2 = \frac{x_\eta^2 + y_\eta^2}{\mathbf{J}}, \tag{110}$$

that is, the length of the normal vectors to a boundary are the same as the lengths of the tangent vector to the same boundary divided by the Jacobian, and

$$\vec{N}_1 = \frac{1}{\mathbf{J}} C\,\mathbf{grad}_{\xi,\eta}\xi = \frac{1}{\mathbf{J}} C\,\vec{e}_1, \qquad \vec{N}_2 = \frac{1}{\mathbf{J}} C\,\mathbf{grad}_{\xi,\eta}\eta = \frac{1}{\mathbf{J}} C\,\vec{e}_2, \tag{111}$$

where

$$\vec{e}_1 = \begin{pmatrix}1\\0\end{pmatrix}, \qquad \vec{e}_2 = \begin{pmatrix}0\\1\end{pmatrix}. \tag{112}$$

Thus the normal vectors are scaled columns of the matrix C.

Because the boundary has four parts, the boundary condition (2) has four parts, one of which is

$$\beta(\vec{\mathbf{n}}_1, K\,\mathbf{grad}_{x,y}u) + \alpha u = \gamma, \qquad \xi = 0, 0 \leq \eta \leq 1. \tag{113}$$

Note that the unit outward normal to the boundary $\xi = 0$ (in logical space) is

$$\vec{n}_1 = -e_1. \tag{114}$$

The boundary condition (113) can be written

$$-\beta\left(\frac{1}{|\vec{N}_1|} C\vec{e}_1, K\frac{1}{\mathbf{J}} C\,\mathbf{grad}_{\xi,\eta}\tilde{u}\right) + \alpha\tilde{u} = \gamma, \tag{115}$$

or

$$\frac{\beta}{\mathbf{J}\,|\vec{N}_1|}\left(\vec{e}_1, \frac{1}{\mathbf{J}} C^*KC\,\mathbf{grad}_{\xi,\eta}\tilde{u}\right) + \alpha\tilde{u} = \gamma, \tag{116}$$

or

$$\frac{\beta}{\mathbf{J}\,|\vec{N}_1|}(-e_1, \tilde{K}\,\mathbf{grad}_{\xi,\eta}\tilde{u}) + \alpha\tilde{u} = \gamma, \tag{117}$$

or

$$\tilde{\beta}(\vec{n}_1, \tilde{F}) + \tilde{\alpha}\tilde{u} = \tilde{\gamma}, \tag{118}$$

where

$$\begin{aligned} \tilde{F} &= \tilde{K}\,\mathbf{grad}_{\xi,\eta}\tilde{u}, \\ \tilde{\alpha}(\xi,\eta) &= \alpha(x(\xi,\eta), y(\xi,\eta)), \\ \tilde{\beta} &= \frac{\beta(x(\xi,\eta), y(\xi,\eta))}{\mathbf{J}(\xi,\eta)\,|\vec{N}_1|}, \\ \tilde{\gamma}(\xi,\eta) &= \gamma(x(\xi,\eta), y(\xi,\eta)). \end{aligned} \tag{119}$$

The important point here is that the transformed PDE multiplied by the Jacobian, and the BC multiplied by the Jacobian or not, have the same form as the original PDE and BC. Consequently, the support-operator method for a rectangular grid can be applied to the transformed problem. Thus $\mathbf{div}_{\xi,\eta}$ becomes the prime operator, $\mathbf{grad}_{\xi,\eta}$ becomes the derived operator, and $\tilde{K}$ becomes the matrix.

To measure the size of the solution and the fluxes, or the errors in these quantities, it is most appropriate to use invariant inner products:

$$\begin{aligned} \langle \tilde{u}, \tilde{v} \rangle &= \int_0^1\int_0^1 \tilde{u}\tilde{v}\,\mathbf{J}\,d\xi\,d\eta, \\ \langle \tilde{F}, \tilde{G} \rangle &= \int_0^1\int_0^1 (\mathcal{J}^*\tilde{F}, \mathcal{J}^*\tilde{G})\frac{1}{\mathbf{J}}\,d\xi\,d\eta, \end{aligned} \tag{120}$$

where $(\cdot,\cdot)$ is the standard inner product of vectors.

5.1. *The Combined Method*

To combine the methods, first the mapping method is applied to a given problem and then the support-operators method is applied to the transformed problem. Thus, in the description of the support-operators method, x and y must be replaced by ξ and η so that, in logical space, the grid is given by

$$\xi_i = \frac{i-1}{N-1}, 1 \leq i \leq N, \qquad \eta_j = \frac{j-1}{M-1}, 1 \leq i \leq N, \tag{121}$$

and then the grid spacing in logical space is given by $h\xi = 1/(N-1)$, and $h\eta = 1/(M-1)$. In physical space, the grid is given by

$$X_{(i,j)} = x(\xi_i, \eta_j), Y_{(i,j)} = y(\xi_i, \eta_j), \qquad 1 \leq i \leq N, 1 \leq i \leq N. \tag{122}$$

Scalar functions are invariant objects, so the same notation for discrete functions values can be used in both logical and physical space. However, discrete vectors have different components in logical space and physical space. In logical space the vector $\vec{A}$ has components $(A\xi, A\eta)$ that are the same as those described in Section 3.2, that is, $A\xi_{(i,j)}$ is located at the center of the left vertical side of logical cell (i, j) while $A\eta_{(i,j)}$ is located at the center of the bottom side of logical cell (i, j). In physical space, the components are described as in Section 4, "Support Operators on General Grids."

Because the mapping method preserves the form of the boundary-value problem and the support-operators algorithm has the desired properties on rectangular grids, the discretized problem will involve a symmetric positive-definite matrix that is given in terms of a nearest neighbor stencil. Such discretizations have been called mimetic [4] in the literature. The accuracy is checked numerically in the next section.

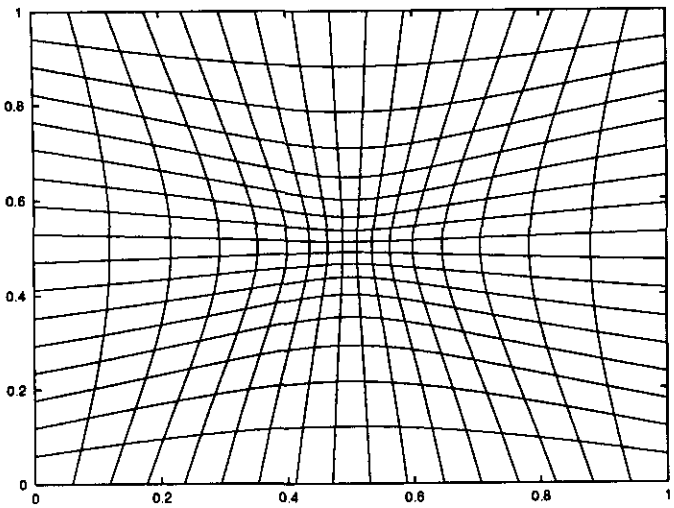

FIG. 18. Grid on a square with $\varepsilon = 10$.

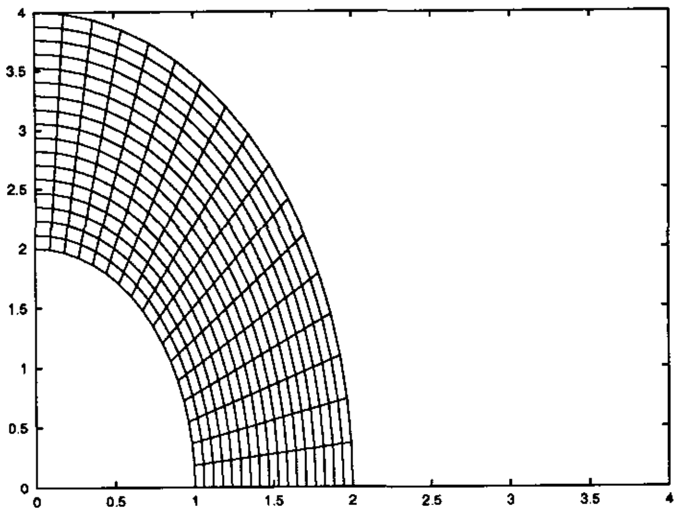

FIG. 19. Elliptical grid with $a = 2$.

6. NUMERICAL TESTS

Background material on numerically testing finite-difference algorithms can be found in Roache [8], Knorr *et al.* [5], Gupta [3], and Perrone and Kao [7]. Numerical tests are performed only for the combined method. The errors in the numerical scheme are measured in both the maximum and mean square norms for both the solution and the fluxes. The norms are discrete analogs of the invariant norms given by the inner products defined in (120). Thus, if $U_{(i,j)}$ is a function defined on the grid, then define

$$\|U\|_\infty = \max_{i=1}^{N-1} \max_{j=1}^{M-1} |U_{(i,j)}|, \qquad \|U\|_2^2 = \sum_{i=1}^{N-1} \sum_{j=1}^{M-1} U_{(i,j)}^2 \mathbf{J}_{(i,j)} h\xi h\eta, \tag{123}$$

where $\mathbf{J}_{(i,j)} = \mathbf{J}(\xi_i, \eta_j)$.

If $\vec{W} = (W\xi, W\eta)$ is a flux defined on the grid, recall that it is defined on the cell faces, so first define the cell-centered quantities

$$\vec{W}_{(i,j)} = \left(\frac{W\xi_{i,j} + W\xi_{i+1,j}}{2}, \frac{W\eta_{i,j} + W\eta_{i+1,j}}{2}\right) \tag{124}$$

and then define the vector

$$\vec{F}_{(i,j)} = \frac{1}{\mathbf{J}_{(i,j)}} \vec{K}_{(i,j)} \vec{W}_{(i,j)}, \tag{125}$$

where $\vec{F} = (FX, FY)$. Now the norms are given by

$$\|\vec{W}\|_\infty = \max_{i=1}^{N-1} \max_{j=1}^{M-1} (\max(|FX_{(i,j)}|, |FY_{(i,j)}|)), \tag{126}$$

$$\|\vec{W}\|_2^2 = \sum_{i=1}^{N-1} \sum_{j=1}^{M-1} (\vec{F}X_{(i,j)}^2 + \vec{F}Y_{(i,j)}^2)\mathbf{J}_{(i,j)} h\xi h\eta.$$

Recall that the grid points are given by

$$X_{(i,j)} = x(\xi_i, \eta_j), \qquad Y_{(i,j)} = y(\xi_i, \eta_j). \tag{127}$$

If u is an exact solution, then define

$$u_{(i,j)} = u(X_{(i,j)}, Y_{(i,j)}), \tag{128}$$

while if $\vec{w} = (w\xi, w\eta)$ is an exact flux given in logical coordinates then define the cell-face-centered components of the

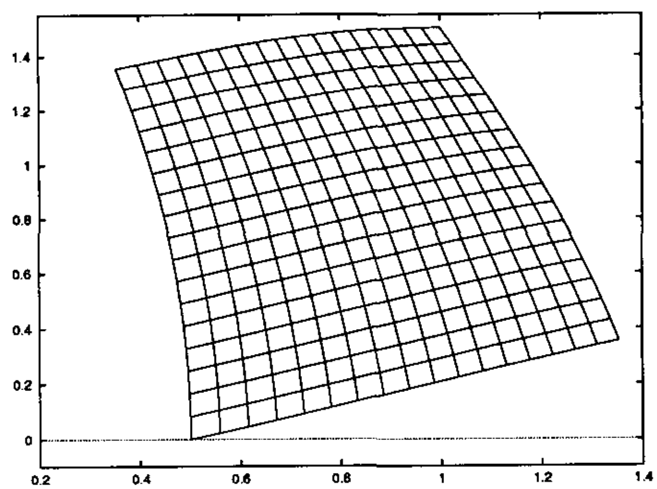

FIG. 20. Curvilinear grid with $\varepsilon = 0.500$.

TABLE II

Uniform Grid

N order:	Max order	Mean order	Max const 2	Mean const 2	Max order	Mean order	Max const 1	Mean const 1.5
9			.93	.61			0.39	0.68
17	2.1	2.0	.92	.59	1.80	1.9	0.20	0.46
33	2.0	2.0	.92	.58	1.50	1.9	0.14	0.34
65	2.0	2.0	.92	.58	0.64	1.8	0.18	0.27
129	2.0	2.0	.92	.58	0.75	1.7	0.21	0.23
257	2.0	2.0	.92	.57	0.88	1.6	0.22	0.21

flux by

$$w\xi_{(i,j)} = w\xi\left(\xi_i, \eta_j + \frac{h\eta}{2}\right), \qquad w\eta_{(i,j)} = w\eta\left(\xi_i + \frac{h\xi}{2}, \eta_j\right). \tag{129}$$

Now the errors in an approximate solution U with flux $\vec{W} = (W\xi, W\eta)$ are given by

$$\begin{aligned} E_\infty(U) &= \|u - U\|_\infty, \\ E_2(U) &= \|u - U\|_2, \\ E_\infty(\vec{W}) &= \|\vec{\tilde{w}} - \vec{W}\|_\infty, \\ E_2(\vec{W}) &= \|\vec{\tilde{w}} - \vec{W}\|_2. \end{aligned} \tag{130}$$

In the numerical test, $M = N = 2^r + 1$ and $h = 2^{-r} = 1/(M - 1)$. If E^h is any one of the norms of errors given in (130) for a grid with M points, then it is expected that $E^h \approx Ch^k$ where C and k are constants and h is sufficiently small. To test this numerically, note that

$$\frac{E^{(r)}}{E^{(r+1)}} \approx \frac{C(1/2^r)^k}{C(1/2^{(r+1)})^k} = 2^k, \tag{131}$$

for r sufficiently large. Consequently, the order k of the error is defined by

$$k = \lim_{r\to\infty} \log_2 \frac{E^{(r)}}{E^{(r+1)}}. \tag{132}$$

Once the order has been computed, then the error constant is given by

$$C = \lim_{r\to\infty} (M-1)^k E^{(r)} = \lim_{r\to\infty} 2^{kr} E^{(r)}. \tag{133}$$

A test problem is created by first choosing K to be a rotation of a diagonal matrix:

$$K = RDR^*, \tag{134}$$

where

$$R = \begin{pmatrix} +\cos(\theta) & -\sin(\theta) \\ +\sin(\theta) & +\cos(\theta) \end{pmatrix}, \qquad D = \begin{pmatrix} d_1 & 0 \\ 0 & d_2 \end{pmatrix}. \tag{135}$$

TABLE III

Square with $\varepsilon = 5$

N order:	Max order	Mean order	Max const 2	Mean const 2	Max order	Mean order	Max const 1	Mean const 1.5
9			3.1	1.8			1.60	2.00
17	2.0	2.1	3.1	1.7	1.60	1.8	.98	1.50
33	2.0	2.1	3.2	1.7	1.10	1.8	.92	1.20
65	2.0	2.0	3.2	1.6	.81	1.7	1.00	1.00
129	2.0	2.0	3.2	1.6	88	1.6	1.10	.94
257	2.0	2.0	3.2	1.6	95	1.5	1.20	.91

TABLE IV

Square with $\varepsilon = 10$

N order:	Max order	Mean order	Max const 2	Mean const 2	Max order	Mean order	Max const 1	Mean const 1.5
9			6.0	3.9			2.8	3.8
17	2.0	2.1	6.2	3.5	1.40	1.6	2.0	3.3
33	2.0	2.1	6.4	3.3	.84	1.6	2.2	3.0
65	2.0	2.0	6.4	3.2	.82	1.6	2.5	2.8
129	2.0	2.0	6.5	3.2	.93	1.6	2.6	2.6
257	2.0	2.0	6.5	3.2	1.00	1.5	2.6	2.6

and

$$\theta = \frac{3\pi}{12},$$

$$d_1 = 1 + 2x^2 + y^2, \tag{136}$$

$$d_2 = 1 + x^2 + 2y^2.$$

The solution to the PDE is chosen to be

$$u(x, y) = \sin(\pi x)\sin(\pi y), \tag{137}$$

and the f is computed from the PDE (1). Boundary conditions of the form

$$(K\vec{w}, \vec{n}) + \alpha u = \gamma, \tag{138}$$

where

$$\alpha = \frac{e^{xy+x+y}}{\sin(x)\cos(y) + (x+y)^2 2^2}, \tag{139}$$

are implemented. Now γ can be computed from the boundary condition (138). (In the code, the boundary conditions are multiplied by the denominator of α.) This provides a complete description of the problem used to test the algorithm.

Several grids were used with this test problem. The first class of grids were given by mapping of the unit square to the unit square (see Fig. 18):

$$x = \xi + \varepsilon\xi(1-\xi)(\tfrac{1}{2}-\xi)\eta(1-\eta),$$
$$y = \eta + \varepsilon\eta(1-\eta)(\tfrac{1}{2}-\eta)\xi(1-\xi). \tag{140}$$

The second class of mappings were given by elliptical coordinates (see Fig. 19):

$$x = r\cos(\theta), \qquad y = ar\sin(\theta), \tag{141}$$

where

$$r = 1 + \xi, \qquad \theta = \frac{\pi\eta}{2}. \tag{142}$$

When $a = 1$, this gives polar coordinates. In this and only this case, the grid is orthogonal. The final mapping gives a general

TABLE V

Elliptical with $a = 1$ (Polar)

N order:	Max order	Mean order	Max const 2	Mean const 2	Max order	Mean order	Max const 1	Mean const 1.75
9			1.1	.63			1.8	4.7
17	1.8	2.0	1.3	.60	1.7	1.9	1.1	3.7
33	1.9	2.0	1.3	.59	1.3	2.0	0.83	3.0
65	2.0	2.1	1.4	.59	1.2	2.0	0.72	2.5
129	2.0	2.0	1.4	.58	1.1	1.9	0.66	2.2
257	2.0	2.0	1.4	.58	1.0	1.8	0.64	2.1

TABLE VI

Elliptical with $a = 2$

N order:	Max order	Mean order	Max const 2	Mean const 2	Max order	Mean order	Max const 1	Mean const 1.75
9			15.	17.			170.	650.
17	2.0	2.1	15.	15.	1.40	1.7	120.	610.
33	1.8	2.1	17.	15.	1.90	2.0	63.	600.
65	1.9	2.0	19.	14.	2.00	1.9	32.	430.
129	1.9	2.0	20.	14.	1.80	2.0	18.	370.
257	2.0	2.0	20.	14.	.65	1.9	22.	330.

grid (see Fig. 20):

$$x = \xi + \varepsilon \cos\left(\frac{\pi}{4}(\xi + \eta)\right); \qquad y = \eta + \varepsilon \sin\left(\frac{\pi}{4}(\xi + \eta)\right). \tag{143}$$

6.1. *Data*

Data were collected for $M = 2^r + 1$ for $r = 3, ..., 8$. All results were tabulated with two significant digits. The first column in the tables give the number of points in the grid. The next four columns give the data for the solution, while the last four columns give the data for the fluxes. The columns labeled "max order" and "mean order" give the order of the method as determined using (132), while the columns labeled "max const" and "mean const" give the error constants as determined by (133).

Table II gives the base case of a uniform grid (say (140) with $\varepsilon = 0$). Tables III and IV give the data for the mapping of the square to the square shown in Fig. 18. Tables V and VI give the data for the elliptical grids shown in Fig. 19. Finally, Tables VII and VIII give the data for the general non-orthogonal grid shown in Fig. 20.

In all test problems, the order of convergence of the solution in the maximum and mean-square norm is 2. The mean-norm orders of convergence for the fluxes vary between 1.5 and 1.75 for examples with non-trivial mappings, while in the maximum norm the order is 1.0 when non-trivial mappings are used. A number of other tests were run, for example, problems where d_1 and d_2 in (136) were more complicated and where the solution u (137) had higher order polynomial terms added. For this more complicated example, Dirichlet boundary conditions and a case where three sides of the region had Neumann and one side had Dirichlet boundary conditions were also run. The conclusions hold also for these tests, except that for some cases the order of convergence for the fluxes was a bit lower than for those presented, or was unexpectedly high. For some examples the grids were not fine enough, so the asymptotic limit had not been reached.

For all of the regions, when the parameters of the mapping are changed the order of convergence for all measures of the error remain unchanged. For the mapping of the square to the square, changing $\varepsilon = 5$ to $\varepsilon = 10$ makes a nontrivial change to the grid, but the convergence constants change by at most a factor of 2, the same as for the change in ε. For the elliptical grids, changing $a = 1$ to $a = 2$ causes increases in the error constant, at the highest resolutions, by factors ranging from 14 to 160. This is presumably true because the grid for $a = 1$ is orthogonal, while the grid for $a = 2$ is not. Again, for the general grid, changing $\varepsilon = 0.25$ to $\varepsilon = 0.5$ makes a significant change in the grid. As with the grid on the square, the convergence constants increase by at most a factor of 2.

The linear equations were solved using an SOR solver with

TABLE VII

General Transformation with $\varepsilon = 0.250$

N order:	Max order	Mean order	Max const 2	Mean const 2	Max order	Mean order	Max const 1	Mean const 1.75
9			1.1	.63			1.08	2.3
17	2.0	2.0	1.1	.61	2.00	2.0	.53	1.9
33	2.0	2.0	1.1	.60	1.70	2.0	.31	1.5
65	1.9	2.1	1.1	.59	1.30	1.9	.25	1.3
129	2.0	2.0	1.1	.59	.83	1.8	.28	1.2
257	2.0	2.0	1.1	.58	.87	1.7	.31	1.3

TABLE VIII

General Transformation with $\varepsilon = 0.500$

N order:	Max order	Mean order	Max const 2	Mean const 2	Max order	Mean order	Max const 1	Mean const 1.75
9			1.1	.63			1.80	4.7
17	1.8	2.0	1.3	.60	1.7	2.0	1.10	3.7
33	1.9	2.0	1.3	.59	1.3	2.0	.80	3.0
65	2.0	2.1	1.4	.59	1.2	2.0	.70	2.5
129	2.0	2.0	1.4	.58	1.1	1.9	.66	2.2
257	2.0	2.0	1.4	.58	1.0	1.8	.64	2.1

a relaxation factor of 1.8. The iterations were stopped when the residual was less than 10^{-8} or the number of iterations exceeded 10^4. The SOR solver required slightly less than some constant times M^2 iterations to solve the linear equations. Clearly, faster solvers will be a great advantage for problems with even modest values of M.

REFERENCES

1. B. Das, T. H. Robey, S. Steinberg, and D. Zhang, *Math. and Computers in Simulation* **36,** 57 (1994).
2. B. Das, S. Steinberg, and S. Weber, *Transport in Porous Media,* in press (1995).
3. M. M. Gupta, *A Fourth Order Finite Difference Scheme for Two-Dimensional Elliptic Equations,* Scientific Computing, edited by R. Stepelman *et al.* (IMACS/North-Holland, Amsterdam, 1983).
4. J. M. Hyman, R. J. Knapp, and J. C. Scovel, *Physica D* **60,** 112 (1992).
5. G. Knorr, G. Joyce, and A. J. Marcus, *J. Comput. Phys.* **38,** 227 (1980).
6. P. M. Knupp and S. Steinberg, *The Fundamentals of Grid Generation* (CRC Press, Boca Raton, 1993).
7. N. Perrone and R. Kao, *Comput. and Structures* **5,** 45 (1975).
8. P. J. Roache, A method for uniform reporting of grid refinement studies, in *Symposium of Quantification of Uncertainty in Computational Fluid Dynamics, ASME Fluids Engineering Division Summer Meeting, Washington, DC, June 1993.*
9. A. Favorskii, A. Samarskii, M. Shashkov, and V Tishkin, *Differential Equations* **17,** 854 (1981).
10. A. Favorskii, T. Korshiya, M. Shashkov, and V. Tishkin, *USSR Comput. Math. and Math. Phys.* **20,** 135 (1980).
11. G. Strang and G. J. Fix, *An Analysis of the Finite Element Method,* Prentice–Hall, Englewood Cliffs, 1973.
12. J. F. Thompson, Z. U. A. Warsi, and C. W. Mastin, *Numerical Grid Generation: Foundations and Applications* (North-Holland/Elsevier, New York, 1985).
13. M. Vinokur, *J. Comput. Phys.* **81,** (1989), 1–52.